

Production of dibaryon $d_{N\Omega}$ in kaon induced reactions

Jing Liu^{1,*}, Qi-Fang Lü^{2,3,4,†}, Chun-Hua Liu^{1,‡}, Dian-Yong Chen^{1,5,§} and Yu-Bing Dong^{6,7,¶}

¹*School of Physics, Southeast University, Nanjing 210094, China*

²*Department of Physics, Hunan Normal University, and Key Laboratory of Low-Dimensional Quantum Structures and Quantum Control of Ministry of Education, Changsha 410081, China*

³*Key Laboratory for Matter Microstructure and Function of Hunan Province, Hunan Normal University, Changsha 410081, China*

⁴*Research Center for Nuclear Physics (RCNP), Ibaraki, Osaka 567-0047, Japan*

⁵*Lanzhou Center for Theoretical Physics, Lanzhou University, Lanzhou 730000, P. R. China*

⁶*Institute of High Energy Physics, Chinese Academy of Sciences, Beijing 100049, China*

⁷*School of Physical Sciences, University of Chinese Academy of Sciences, Beijing 101408, China*

(Dated: December 9, 2022)

In this work, we propose to investigate the $d_{N\Omega}$ dibaryon production in the process $K^-p \rightarrow d_{N\Omega}\bar{\Xi}^0$ by utilizing the kaon beam with the typical momentum to be around 10 GeV, which may be available at COMPASS, OKA@U-70 and SPS@CERN. The cross sections for $K^-p \rightarrow d_{N\Omega}\bar{\Xi}^0$ are estimated and in particular, the cross sections for three kinds of form factor can reach up to 577.20, 5625.51 and 251.11 μb at $P_K = 20$ GeV, respectively. Considering that $d_{N\Omega}$ dominantly decay into $\Xi\Lambda$ and $\Xi\Sigma$, we also estimate the cross sections for $K^-p \rightarrow \Xi^0\Lambda\bar{\Xi}^0$ and $K^-p \rightarrow \Xi^-\Sigma^+\bar{\Xi}^0$, when $P_K = 20$ GeV, where the dibaryon $d_{N\Omega}$ can be observed in the invariant mass distributions of $\Xi^0\Lambda$ and $\Xi^-\Sigma^+$, respectively.

I. INTRODUCTION

Dibaryon is a sort of particles composed of two baryons. As a typical dibaryon, a deuteron consists of one proton and one neutron with a binding energy to be $E_b = 2.22$ MeV. Besides the deuteron, Searching for the dibaryon states composed of other baryons became an intriguing topic of hadron physics in recent decades with the developments of experimental techniques and the accumulations of experimental data.

The theoretical investigations of the dibaryon could date back to the year of 1964, when the dibaryon states were studied by Dyson and Xuong [1] with SU(6) theory, and then in 1977 Jaffe predicted the existence of the H and H^* particles with strangeness $S = -2$, which could be the bound state of $\Lambda\Lambda$ and $\Sigma\Sigma$, respectively. The investigations in two different hadron quark models indicated that there should exist dibaryon states with strangeness to be -3 , which were stable for strong decay [2]. And later, the mass spectrum of the low-lying dibaryons with strangeness to be -1 were evaluated in the quark model [3]. Then some other models had been extended to study the dibaryons, for examples, the quark-cluster model [4], Skyrme Model [5], quark potential model [6], the chiral SU(3) quark model [7], quark delocalization and color screening model [8–12] and realistic phenomenological nucleon-nucleon interaction models [13, 14]. In these model, a series of dibaryon states have been investigated, such as the nonstrange dibaryon d^* with $I(J^P) = 0(3^+)$, dibaryons composed of $N\Xi'$, $N\Xi_c$, $N\Xi_{cc}$, $\Xi_{cc}\Xi_{cc}$ [13, 14], $N\Omega$ and $\Delta\Omega$ [15].

On the experimental side, the first breakthrough was the observations of $d^*(2380)$, which was firstly observed in the cross sections for $np \rightarrow d\pi\pi$ by CELSIUS/WASA Collab-

oration in 2009 [16]. Since the discovery of $d^*(2380)$ in the experiment, that $d^*(2380)$ state has received much more attention. With much better statistics and precision data sample, the WASA-at-COSY Collaboration found that the observed angular distributions for the deuterons and pions of the process $np \rightarrow d\pi^0\pi^0$ in the center-of-mass system clearly preferred $J = 3$ [17, 18], and then the $I(J^P)$ quantum numbers were determined to be $0(3^+)$. Later on, the properties of $d^*(2380)$ had been investigated in various unpolarized np collision processes with more precise data samples, for example, $np \rightarrow np\pi^0\pi^0$, $np \rightarrow pp\pi^0\pi^-p$, $np \rightarrow d\pi^0\pi^0$ [19–21], and polarized np scattering process [22].

After the experimental observations of $d^*(2380)$, it has attracted a lot of theorists' attentions to explore its exotic nature [23–30]. However, there were also some different views, for example, in Refs. [31–33], the authors found that the peak structure corresponding to $d^*(2380)$ could be tied to a triangle singularity in the last step of the reaction. No matter what the nature of $d^*(2380)$ is, the experimental breakthrough indeed stimulated theorists' interests in dibaryons states. Some dibaryon states had been investigated in various models. For examples, in a three-body hadronic model, the authors in Ref. [34] calculated the $N\Delta$ and $\Delta\Delta$ dibaryon states. In the one pion exchange potential model, the H -like $\Lambda_c\Lambda_c$ [35], $\Lambda_c N$ [36] dibaryons were researched. The possible $\Lambda_c\Lambda_c/\Lambda_b\Lambda_b$ [37], and $N\Sigma_{c,b}$ [38] dibaryon states were studied in the quark delocalization color screening model, and the possible $\Delta^0\Delta^0$, $\Omega\Omega$, $\Xi\Xi$ dibaryons were investigated in Refs. [39–43].

As for the dibaryon states with strangeness $S = -3$, the possibilities of the existence of such kind of dibaryons have been evaluated by various model. For example, the estimations in Ref. [44] indicated that there might exist two bound states $N\Omega$ and $\Delta\Omega$ dibaryons, respectively, and in Ref. [15], the authors found that the $N\Omega$ and $\Delta\Omega$ were weakly bound systems in the chiral quark model. The QCD sum rule estimations in Ref. [45] indicate that the $N\Omega$ dibaryon with $J^P = 2^+$ was stable for strong decay. In Ref. [46], the HAL QCD Collaboration calculated the $N\Omega$ potential in $2 + 1$ flavor Lattice

*Electronic address: jingliu@seu.edu.cn

†Electronic address: lvqifang@hunnu.edu.cn

‡Electronic address: liuch@seu.edu.cn

§Electronic address: chendy@seu.edu.cn

¶Electronic address: dongyb@ihep.ac.cn

QCD and one bound state with the spin and the binding energy to be about 20 MeV was found. In the year of 2019, the HAL QCD Collaboration updated their estimations of Ref. [46] near the physical point and they found the binding energy of the $p\Omega(^5S_2)$ became $2.46(0.34)^{(+0.04)}_{(-0.11)}$ MeV. Simulated by the most recent Lattice QCD estimations, the authors in Ref. [47] estimated the productions of the Ω -dibaryons by utilizing a dynamical coalescence mechanism for the relativistic heavy-ion collisions, and the strong decays of $d_{N\Omega}$ into conventional hadrons were evaluated [48].

Actually, experimentally producing the dibaryon $d_{N\Omega}$ is the first step of investigating its properties. Thus, searching $d_{N\Omega}$ experimentally becomes a pressing task. The key point of producing $d_{N\Omega}$ dibaryon is the production of Ω baryon. In the high energy heavy-ion collision or pp collision processes, a large quantity of quarks with different flavors can be produced, where three strange quarks have chance to form a Ω baryon and produce a $d_{N\Omega}$ dibaryon by interacting with a nucleon. In the year of 2018, the STAR Collaboration at RHIC investigated the proton- Ω interaction by measuring the corresponding correlation function in heavy-ion collisions at $\sqrt{s_{NN}} = 200$ GeV [49]. By comparing the measured correlation ratio with the theoretical calculations, they concluded that the measurements slightly favored a proton- Ω bound system with a binding energy of 27 MeV [49]. Similarly, the ALICE Collaboration also proposed to investigate the strong interaction among hadrons, including proton- Ω , by using the ultrarelativistic proton-proton collisions at LHC [50].

Besides the high energy heavy-ion collision and pp collision processes, the Ω baryon can also be produced by kaon induced reactions since there is already a strange quark in the kaon. In Ref. [51], a project of the extension of the Hadron Experimental Facility at J-PARC was proposed. By utilizing the secondary beam of kaon with the typical momentum to be around 3 GeV, the Ω baryon can be produced via the $K^-p \rightarrow \Omega^- K^+ K^{(*)0}$ reaction and then the dibaryon $d_{N\Omega}$ can be investigated in the invariant mass spectrum of $\Xi^- \Lambda$ of the process $\Omega^- d \rightarrow \Xi^- \Lambda p$.

In addition to the secondary beam of kaon at J-PARC [52], the high energy kaon beam with high quality are also available at COMPASS [53], OKA@U-70 [54] and SPS@CERN [55]. These high energy beam, especially ones with momentum to be around 10 GeV, may provide us another approach to directly produce $d_{N\Omega}$ via the reaction $K^-p \rightarrow d_{N\Omega} \Xi^0$ and then the $d_{N\Omega}$ can decay into $\Xi \Lambda$ and $\Xi \Sigma$. Thus, one can detect $d_{N\Omega}$ in the $\Xi \Lambda$ and $\Xi \Sigma$ invariant mass spectra of the processes $K^-p \rightarrow \Xi^0 \Xi \Lambda$ and $K^-p \rightarrow \Xi^0 \Xi \Sigma$, respectively. In the present work, we evaluate the possibility of observing $d_{N\Omega}$ dibaryon in these processes by estimating their cross sections.

This work is organized as follows. After the introduction, the mechanism of $d_{N\Omega}$ production in kaon induced reactions is presented. In Section III, the cross sections for the processes $K^-p \rightarrow d_{N\Omega} \Xi^0$, $K^-p \rightarrow \Xi^0 \Lambda \Xi^0$ and $K^-p \rightarrow \Xi^- \Sigma^+ \Xi^0$ are presented, and the last section is devoted to a short summary.

II. PRODUCTION MECHANISM OF $d_{N\Omega}$

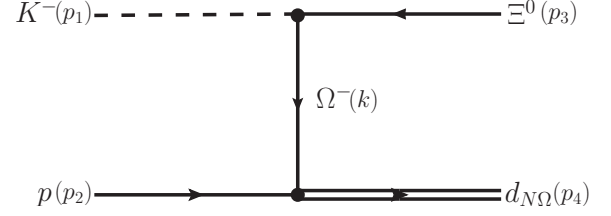


FIG. 1: Diagram contributing to the process of $K^-p \rightarrow d_{N\Omega} \Xi^0$, where the $d_{N\Omega}$ is considered as a S-wave $N\Omega$ dibaryon with $J^P = 2^+$.

In the present work, we consider the $d_{N\Omega}$ is a dibaryon composed of N and Ω with the $J^P = 2^+$. The dibaryon $d_{N\Omega}$ can be produced in the high energy K^-p interaction process. Empirically, in high energy K^-p scattering process, the contributions from the s and u channels are much smaller than the one from t channel [56–59], thus the $d_{N\Omega}$ production in high energy K^-p scattering can occur dominantly by exchanging a Ω baryon as presented in Fig. 1. Here, we estimated the cross sections for $K^-p \rightarrow d_{N\Omega} \Xi$ in an effective Lagrangian approach. The interaction of the dibaryon $d_{N\Omega}$ and its components can be described as [48],

$$\mathcal{L}_{d_{N\Omega}N\Omega} = g_{d_{N\Omega}N\Omega} d_{N\Omega}^{\mu\nu} \bar{\Omega}_\mu \gamma_\nu N^c + H.c., \quad (1)$$

where $N^c = C\bar{N}^T$, $\bar{N}^c = N^T C$, and $C = i\gamma^2\gamma^0$ is the charge-conjugation matrix, T is the transpose transformation operator. The effective Lagrangian for $\Omega\Xi K$ interaction reads [60–65],

$$\mathcal{L}_{\Omega\Xi K} = \frac{g_{\Omega\Xi K}}{m_\pi} \partial_\beta K \bar{\Omega} \gamma^\beta \Xi + H.c.. \quad (2)$$

With the above effective Lagrangians, we can obtain the amplitude corresponding to Fig. 1, which is,

$$\mathcal{M} = \frac{g_{\Omega\Xi K}}{m_\pi} (-ip_1^\beta) g_{d_{N\Omega}N\Omega} d_{N\Omega}^{\mu\nu} F(k^2, m_\Omega) \times [\bar{u}^c(p_2, m_2) \gamma_\nu S(k, m_\Omega)_{\mu\beta} v(p_3, m_3)], \quad (3)$$

with $S(k, m_\Omega)_{\mu\beta}$ to be the propagator of the Ω baryon, which is,

$$S(k, m_\Omega)_{\mu\beta} = i \frac{k + m_\Omega}{k^2 - m_\Omega^2} \left[-g_{\mu\beta} + \frac{1}{3} \gamma_{\mu\beta} + \frac{2k_\mu k_\beta}{3m_\Omega^2} + \frac{\gamma_\mu k_\beta - \gamma_\beta k_\mu}{3m_\Omega} \right]. \quad (4)$$

To depict the internal structure and the off shell effect of the exchanged Ω baryon, we introduce a form factor $F(k^2, m_\Omega)$ in the amplitude and its concrete form will be discussed later. With the amplitude in Eq. (3), one can obtain the cross section for $K^-p \rightarrow d_{N\Omega} \Xi^0$ by,

$$\frac{d\sigma}{d\cos\theta} = \frac{1}{32\pi s} \frac{|\vec{p}_f|}{|\vec{p}_i|} \left(\frac{1}{2} |\mathcal{M}|^2 \right), \quad (5)$$

where $s = (p_1 + p_2)^2$ is the center of mass energy and θ is the scattering angle, which refers to the angle of outgoing $d_{N\Omega}$ and the kaon beam direction in the center of mass frame. The \vec{p}_i

and \vec{p}_f are three momentum of the initial kaon beam and the final $d_{N\Omega}$ dibaryon in the center of mass frame, respectively.

As indicated in Ref. [48], the dibaryon $d_{N\Omega}$ dominantly decay into $\Lambda\Xi$ and $\Xi\Sigma$. Thus one can detect $d_{N\Omega}$ in the invariant mass spectrum of $\Lambda\Xi^0$ and $\Xi^-\Sigma^+$ of the processes $K^-p \rightarrow \Xi^0\Lambda\Xi^0$ and $K^-p \rightarrow \Xi^-\Sigma^+\Xi^0$, respectively. To depict these processes, additional effective Lagrangians related to $d_{N\Omega}\Xi\Lambda$ and $d_{N\Omega}\Xi\Sigma$ are involved. Since Ξ , Σ and Λ have the same J^P quantum numbers, thus these two effective Lagrangians have the same form, which is,

$$\mathcal{L}_{d_{N\Omega}Y_1Y_2} = i\frac{G_{d_{N\Omega}Y_1Y_2}}{2M_{Y_1}}\bar{Y}_1^c(\gamma_\mu\partial_\nu + \gamma_\nu\partial_\mu)Y_2d_{N\Omega}^{\mu\nu} + \frac{F_{d_{N\Omega}Y_1Y_2}}{(2M_{Y_1})^2}\partial_\mu\bar{Y}_1^c\partial_\nu Y_2d_{N\Omega}^{\mu\nu} + H.c., \quad (6)$$

where Y_1, Y_2 could be Ξ, Σ and Λ . Similar to the case of tensor meson, we can choose $F_{d_{N\Omega}Y_1Y_2} = 0$ with tensor dominance hypothesis [66], and the values of the couplings $G_{d_{N\Omega}Y_1Y_2}$ will be discussed in next section. With this additional effective Lagrangian, we can obtain the amplitudes corresponding to Fig. 2-(a), which are,

$$\begin{aligned} \mathcal{M}_a = & \left[g_{d_{N\Omega}N\Omega}\bar{u}^c(p_2, m_2)\gamma^\nu S(k, m_\Omega)_{\mu\beta}v(p_3, m_3) \right] \left[\frac{g_{\Omega\Xi K}}{m_\pi}(-ip_{1\beta}) \right] \mathcal{P}_{d_{N\Omega}}^{\mu\nu\lambda\omega}(q, m_{d_{N\Omega}}, \Gamma_{d_{N\Omega}}) \\ & \times \left[i\frac{G_{d_{N\Omega}\Xi\Lambda}}{2m_\Xi}\bar{u}^c(p_5, m_5)(\gamma_\lambda(-ip_{4\omega}) + \gamma_\omega(-ip_{4\lambda}))u(p_4, m_4) \right] F(k^2, m_\Omega)F(q^2, m_{d_{N\Omega}}), \end{aligned} \quad (7)$$

where $\mathcal{P}_{d_{N\Omega}}^{\mu\nu\lambda\omega}(q, m_{d_{N\Omega}}, \Gamma_{d_{N\Omega}})$ is the propagator of the dibaryon $d_{N\Omega}$, and its concrete form is,

$$\mathcal{P}_{d_{N\Omega}}^{\mu\nu\lambda\omega}(q, m_{d_{N\Omega}}, \Gamma_{d_{N\Omega}}) = \frac{i}{q^2 - m_{d_{N\Omega}}^2 + im_{d_{N\Omega}}\Gamma_{d_{N\Omega}}} \left[\frac{1}{2}(\tilde{g}_{\mu\lambda}\tilde{g}_{\nu\omega} + \tilde{g}_{\mu\omega}\tilde{g}_{\nu\lambda}) - \frac{1}{3}\tilde{g}_{\mu\nu}\tilde{g}_{\lambda\omega} \right], \quad (8)$$

with $\tilde{g}^{\mu\nu} = -g^{\mu\nu} + q^\mu q^\nu / m^2$. In the above amplitudes, an addition form factor $F(q^2, m_{d_{N\Omega}})$ is introduced to depict the internal structure and off shell effects of the $d_{N\Omega}$ and its concrete form will be discussed in next section. In the same way, one can obtain the amplitude of $K^-p \rightarrow \Xi^0\Xi^-\Sigma^+$ corresponding to Fig. 2-(b). With the amplitudes in Eq. (7), we can obtain the cross sections for the $2 \rightarrow 3$ processes by,

$$d\sigma = \frac{1}{8(2\pi)^4} \frac{1}{\Phi} |\mathcal{M}|^2 dp_5^0 dp_3^0 d\cos\theta d\eta, \quad (9)$$

where $\Phi = 2\sqrt{\lambda(s, m_1^2, m_2^2)} = 4|\vec{p}_1|\sqrt{s}$ with \vec{p}_1 to be the three momentums of the incident particle K^- , p_3^0 and p_5^0 are the energies of the outgoing Ξ^0 and Λ , respectively, in the processes $K^-p \rightarrow \Lambda\Xi^0\Xi^0$ and $K^-p \rightarrow \Xi^0\Xi^-\Sigma^+$.

III. NUMERICAL RESULTS AND DISCUSSIONS

In the present work, we introduce two form factors to depict the internal structures and off-shell effects of the exchanging Ω baryon and internal dibaryon $d_{N\Omega}$. In the literatures, some different kinds of form factors have been employed in the similar estimations. Here we employ three typical types of form factors to discuss the form factor dependences of the cross

sections, which are [67–69],

$$\begin{aligned} F(q^2, m^2) &= \frac{\Lambda^4}{(m^2 - q^2)^2 + \Lambda^4} && \text{Mode I,} \\ F(q^2, m^2) &= \frac{\Lambda^2 - m^2}{\Lambda^2 - q^2} && \text{Mode II,} \\ F(q^2, m^2) &= \exp[-|m^2 - q^2|/\Lambda^2], && \text{Mode III,} \end{aligned} \quad (10)$$

where Λ is a model parameter. In principle, the value of the model parameter Λ should be determined by comparing the theoretical estimations with the corresponding experimental measurements. However, the experimental data for the cross sections for the discussed processes are not available at present. Empirically, the parameter Λ is of order 1 GeV in these three kinds of form factors [67–73]. To investigate the parameter dependences of the cross sections, we use a unique model parameter Λ and vary it from 1.0 to 1.6 GeV in the present work.

Before the estimations of the cross sections for the discussed processes, the relevant coupling constants should be clarified. As for the coupling constant $g_{d_{N\Omega}N\Omega}$, it can be estimated by the compositeness condition of the composite state. In Ref. [48], the coupling constant $g_{d_{N\Omega}N\Omega}$ is estimated to be about 1.88 ~ 2.38 with the variation of the model parameter, where the binding energy is set to be 2.46 MeV. In the present estimation, we take $g_{d_{N\Omega}N\Omega} = 1.97$. With this coupling constant, the partial decay widths of $d_{N\Omega} \rightarrow \Lambda\Xi^0$ and

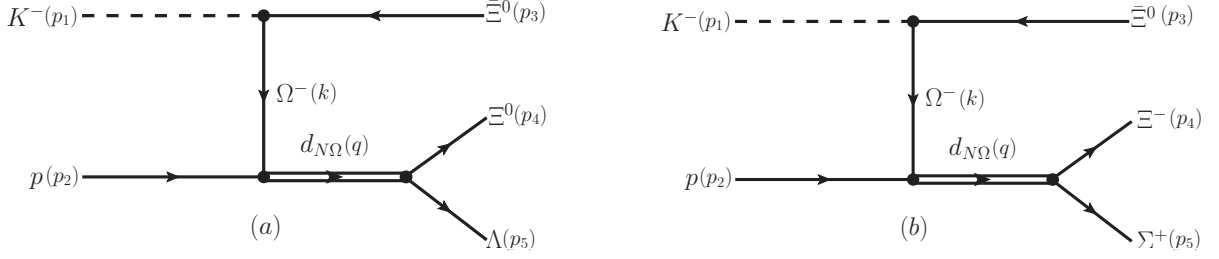


FIG. 2: Diagrams contributing to $K^- p \rightarrow \Xi^0 \Lambda \Xi^0$ (diagram (a)) and $K^- p \rightarrow \Xi^- \Sigma^+ \Xi^0$ (diagram (b)).

$d_{N\Omega} \rightarrow \Sigma^+ \Xi^-$ are estimated to be 582 and 22.8 keV [48], respectively. Together with the effective Lagrangian in Eq. (6), one can obtain amplitudes of $d_{N\Omega} \rightarrow p \Lambda \Xi^0$ and $d_{N\Omega} \rightarrow \Sigma^+ \Xi^-$, and then the partial decay width by,

$$\Gamma_{d_{N\Omega} \rightarrow \dots} = \frac{1}{(2J+1)8\pi} \frac{|\vec{k}_f|}{M_{d_{N\Omega}}^2} |\overline{\mathcal{M}}_{d_{N\Omega} \rightarrow \dots}|^2, \quad (11)$$

where $J = 2$ is the angular momentum of $d_{N\Omega}$, $|\vec{k}_f|$ is the three momentum of the daughter particles in $d_{N\Omega}$ rest frame. From Eq. (11) and the partial widths estimated in Ref. [48], one can estimate the corresponding effective coupling constants, which are $g_{d_{N\Omega} \Lambda \Xi} = 0.21$ and $g_{d_{N\Omega} \Sigma \Xi} = 6.5 \times 10^{-2}$, respectively. As for the coupling constant $g_{K \Xi \Omega}$, we take $g_{K \Xi \Omega} = 2.12$ as in Ref. [65].

With above preparation, we can evaluate the cross sections for $K^- p \rightarrow d_{N\Omega} \Xi^0$ depending on the beam energy and the model parameter Λ in three kinds of form factors as well. Here, we take for typical Λ values in Mode I, Mode II, and Mode III, which are 1.0, 1.2, 1.4, and 1.6 GeV, respectively. The cross sections depending on the beam energy with different Λ with the form factor in Mode I are presented in Fig. 3-(a). From the figure one can find the cross sections for $K^- p \rightarrow d_{N\Omega} \Xi^0$ increase sharply near the threshold of $d_{N\Omega} \Xi^0$, however, when the beam energy is greater than 9 GeV, the cross sections become weakly dependent on the beam energy. In the considered parameter range, the cross sections reach up to $(21.88 \sim 577.20) \mu\text{b}$ at $P_K = 20$ GeV. In addition, we also present the differential cross sections depending on $\cos(\theta)$ in Fig. 3-(b). We select four typical beam energies as examples, which are $P_K = 10, 12, 14, 16$ GeV with $\Lambda = 1.4$ GeV. When $P_K = 10$ GeV, we find the differential cross sections weakly depend on $\cos(\theta)$ in most area but they become rather small at forward angle limit. However, with the increasing of the beam energy, more $d_{N\Omega}$ dibaryon are concentrated in the forward angle area.

The cross sections and differential cross sections for $K p \rightarrow d_{N\Omega} \Xi^0$ estimated with the form factor in Mode II and Mode III are presented in Fig. 4 and 5. The shapes of the cross sections for $K^- p \rightarrow d_{N\Omega} \Xi^0$ obtained with the form factor in Mode-2 and Mode-3 are very similar to that in Mode I, but the magnitudes are a bit difference. In particular, the maximum cross sections of Mode II and Mode III can reach up to 5625.51 and 251.11 μb at $P_K = 20$ GeV, respectively. It is worth nothing to mention that that the cross sections for $K^- p \rightarrow d_{N\Omega} \Xi^0$ in

Mode II are proportional to $(\Lambda^2 - m_\Omega^2)^2$, which will be zero when $\Lambda = m_\Omega$. Since $m_\Omega = 1672.45 \pm 0.29$ MeV, it is understandable that the cross sections with $\Lambda = 1.6$ GeV are much smaller than those with $\Lambda = 1.0, 1.2$ and 1.4 GeV. From Fig. 3-5, one can find the cross sections for $K^- p \rightarrow d_{N\Omega} \Xi^0$ in different modes are of order of 10 μb , which should be large enough to be detected.

Besides the $K^- p \rightarrow d_{N\Omega} \Xi^0$ process, we also estimate the beam energy dependences of the cross sections for $K^- p \rightarrow \Xi^0 \Lambda \Xi^0$ and $K^- p \rightarrow \Xi^- \Sigma^+ \Xi^0$, where $\Xi^0 \Lambda$ and $\Xi^- \Sigma^+$ are the daughter particles of $d_{N\Omega}$. As indicated in Ref. [48], the dibaryon $d_{N\Omega}$ dominantly decays into $\Lambda \Xi^0$, and the branching ratio is estimated to be about 95%, thus one can experimentally detect $d_{N\Omega}$ in the $\Lambda \Xi^0$ invariant mass distributions of the process $K^- p \rightarrow \Xi^0 \Lambda \Xi^0$ as shown in Fig. 2-(a), where Λ can be reconstructed by $p\pi^-$ and $n\pi^0$, while Ξ^0 can be reconstructed by the cascade decay processes $\Xi^0 \rightarrow \Lambda \pi^0 \rightarrow p\pi^-\pi^0$ or $\Xi^0 \rightarrow \Lambda \pi^0 \rightarrow n\pi^0\pi^0$. With the form factor in Mode I, our estimations indicate that the cross sections for $K^- p \rightarrow \Xi^0 \Lambda \Xi^0$ increase sharply near the threshold and then increase very slowly with the increase of the beam energy. In particular, the maximum of the cross section is about 21.74 μb at $P_K = 20$ GeV. Moreover, the branching ratio of $d_{N\Omega} \rightarrow \Xi^- \Sigma^+$ is also sizable, and the final states are charged, which may be easier to be detected. Thus, in the present work, we also estimate the cross sections for $K^- p \rightarrow \Xi^- \Sigma^+ \Xi^0$. As shown in Fig. 2-(b), the beam energy dependences of the cross sections for $K^- p \rightarrow \Xi^- \Sigma^+ \Xi^0$ are very similar to the ones of $K^- p \rightarrow \Xi^0 \Lambda \Xi^0$ and the maximum is about 0.91 μb at $P_K = 20$ GeV.

With the other two form factors in the Mode II and Mode III, we can obtain the cross sections for $K^- p \rightarrow \Xi^0 \Lambda \Xi^0$ and $K^- p \rightarrow \Xi^- \Sigma^+ \Xi^0$, which are presented in Fig. 7 and Fig. 8 in the appendix of the present work. For $K^- p \rightarrow \Xi^0 \Lambda \Xi^0$ in Fig. 7-(a) and Fig. 8-(a) the cross sections are 359.61 and 8.95 μb , respectively. For $K^- p \rightarrow \Xi^- \Sigma^+ \Xi^0$ in Fig. 7-(b) and Fig. 8-(b) the cross sections can reach up to 12.68 and 0.31 μb , respectively.

IV. SUMMARY

The production of the dibaryon $d_{N\Omega}$ is the crucial step of investigating its properties experimentally. The STAR Collaboration at RHIC have detected the dibaryon $d_{N\Omega}$ by measuring

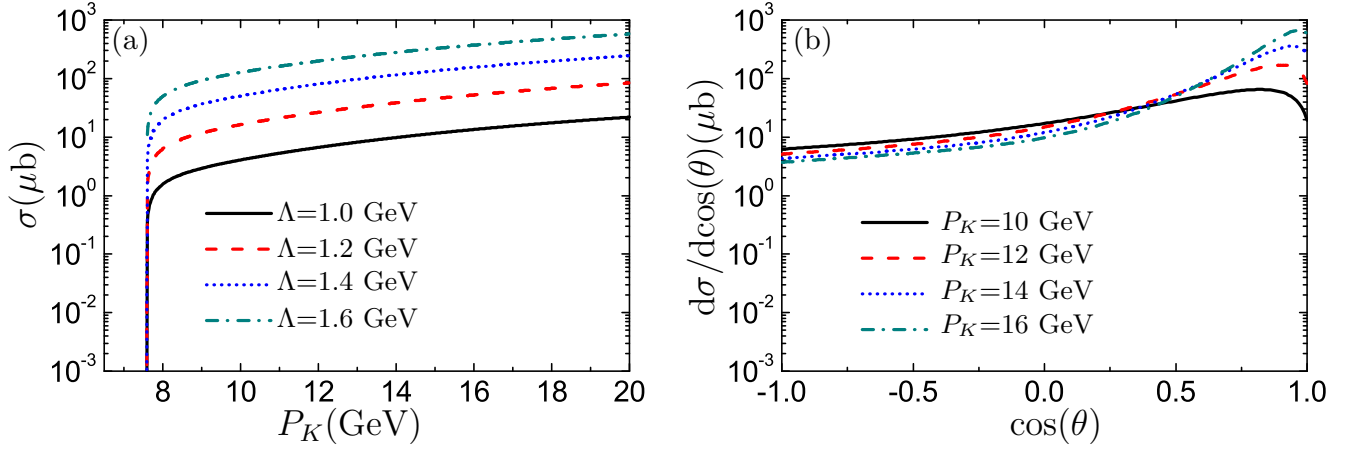


FIG. 3: The cross sections for the process $K^-p \rightarrow d_{N\Omega}\Xi^0$ depending on the beam energy (diagram (a)), and the differential cross sections depending on $\cos(\theta)$ (diagram (b)) with the form factors in Mode I.

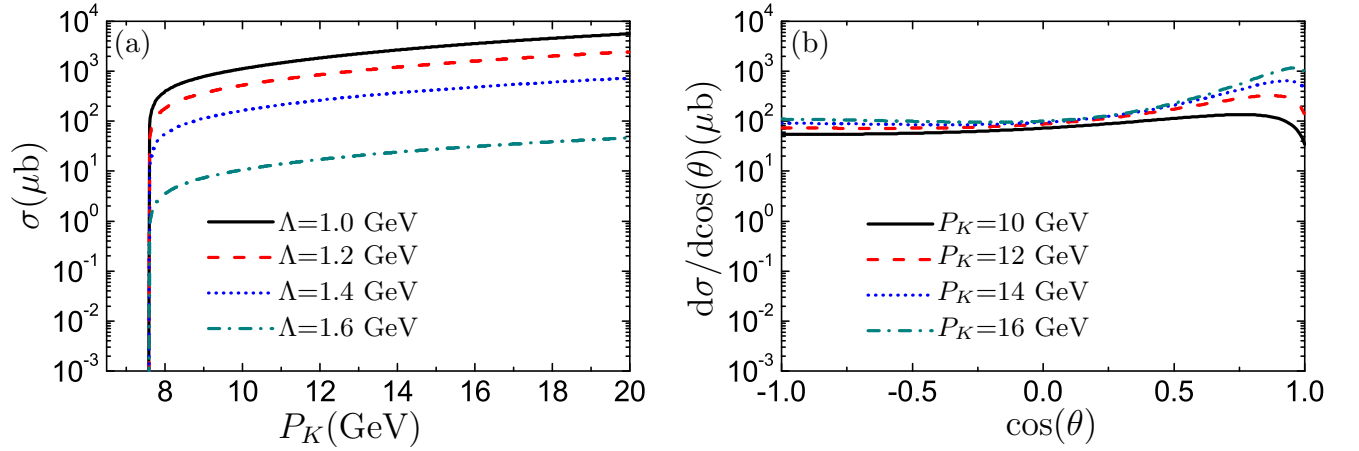


FIG. 4: The same as Fig. 3 but with the form factors in Mode II.

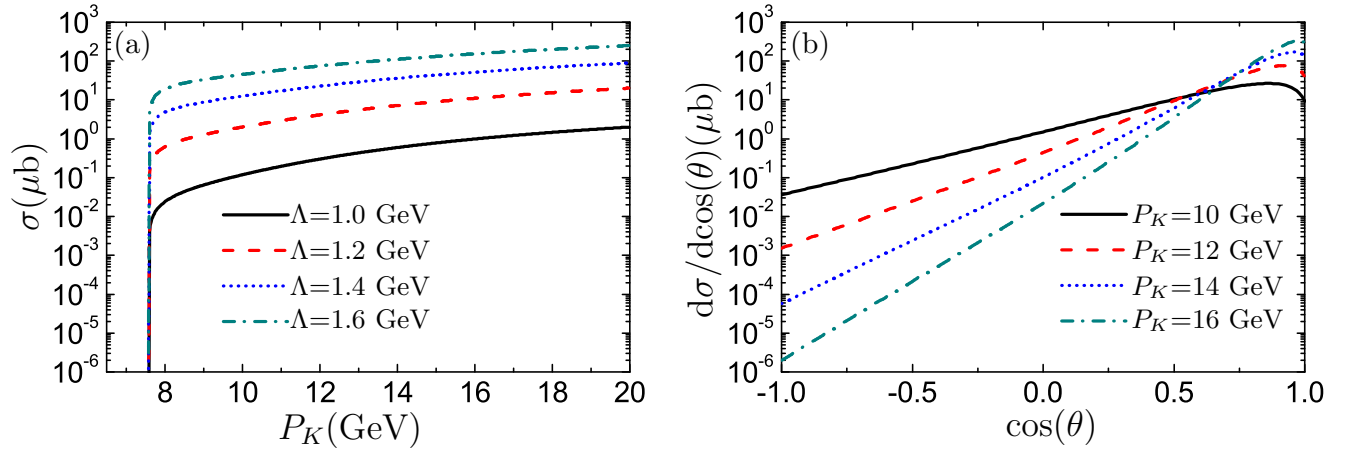


FIG. 5: The same as Fig. 3 but with the form factors in Mode III.

the proton- Ω correlation function in high energy heavy-ion collision. The ALICE Collaboration at LHC also proposed to detect $d_{N\Omega}$ in a very similar processes. By utilizing the secondary kaon beam with the typical momentum to be around 3 GeV, the Hadron experimental Facility at J-PARC proposed to

produce $d_{N\Omega}$ by two step reactions, i.e., $K^-p \rightarrow \Omega^- K^+ K^{(*)0}$, $\Omega d \rightarrow \Xi^- \Lambda p$, where the dibaryon $d_{N\Omega}$ is expected to be observed in the $\Xi^- \Lambda$ invariant mass spectrum.

Besides the above two kinds of production processes, we propose to produce $d_{N\Omega}$ in $K^-p \rightarrow d_{N\Omega}\Xi^0$ process with

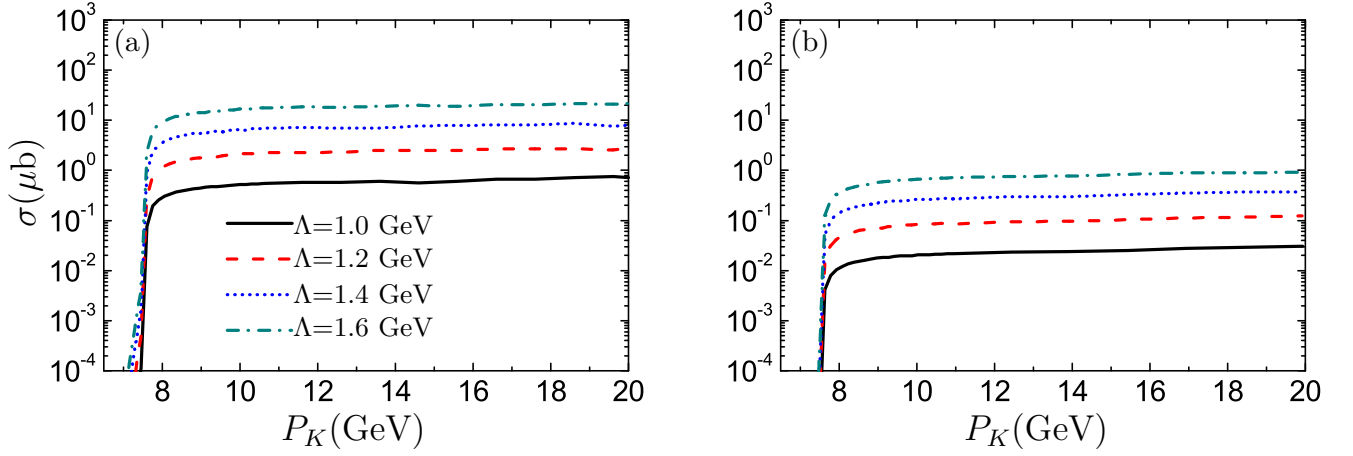


FIG. 6: Cross sections for $K^-p \rightarrow \Xi^0 \Lambda \Xi^0$ (diagram (a)) and $K^-p \rightarrow \Xi^- \Sigma^+ \Xi^0$ (diagram (b)) depending on the beam energy with the form factors in Mode I.

a secondary kaon beam with the typical momentum to be around 10 GeV in the present work. The cross sections for $K^-p \rightarrow d_{N\Omega} \Xi^0$ are estimated and we find the cross section is of the order of $10 \mu b$ at $P_K = 20$ GeV, where different forms of form factors have been employed. Moreover, the estimated differential cross sections indicate that the produced $d_{N\Omega}$ are concentrated in the forward angle area when P_K is greater than 10 GeV.

Considering the fact that $d_{N\Omega}$ dominantly decays into $\Xi \Lambda$, we also estimate the cross sections for $K^-p \rightarrow \Xi^0 \Lambda \Xi^0$ and $K^-p \rightarrow \Xi^+ \Sigma^- \Xi^0$ via $d_{N\Omega}$, where $d_{N\Omega}$ can be detected in $\Xi^0 \Lambda$ and $\Xi^- \Sigma^+$ invariant mass spectrum, respectively. In particular, the cross sections for $K^-p \rightarrow \Xi^0 \Lambda \Xi^0$ are estimated to be $(0.72 \sim 21.74) \mu b$ in Mode I, $(4.31 \sim 359.61) \mu b$ in Mode II, and $(0.04 \sim 8.95) \mu b$ in Mode III.

ACKNOWLEDGEMENTS

This work is supported by the National Natural Science Foundation of China under Grants No.11705056, No. 12175037, No.11947224, No.11475192, No.11975245, and No.U1832173. This work is also supported by the Key Project

of Hunan Provincial Education Department under Grant No. 21A0039, the State Scholarship Fund of China Scholarship Council under Grant No. 202006725011, the Sino-German CRC 110 "Symmetries and the Emergence of Structure in QCD" project by NSFC under the Grant No. 12070131001, the Key Research Program of Frontier Sciences, CAS, under the Grant No. Y7292610K1, and the National Key Research and Development Program of China under Contracts No. 2020YFA0406300.

Appendix A: Cross sections for $K^-p \rightarrow \Xi^0 \Lambda \Xi^0$ and $K^-p \rightarrow \Xi^- \Sigma^+ \Xi^0$ with the form factor in Mode II and Mode III

With the form factor in Mode II and Mode III, we can estimate the cross sections for $K^-p \rightarrow \Xi^0 \Lambda \Xi^0$ and $K^-p \rightarrow \Xi^- \Sigma^+ \Xi^0$, which are presented in Figs. 7 and 8, respectively. Comparing with Fig. 6, one can find the lineshapes of the cross sections obtained with different form factor are very similar but the magnitude of the cross sections are a bit different.

[1] F. Dyson and N. H. Xuong, Phys. Rev. Lett. **13**, no.26, 815-817 (1964) doi:10.1103/PhysRevLett.13.815
[2] J. T. Goldman, K. Maltman, G. J. Stephenson, Jr., K. E. Schmidt and F. Wang, Phys. Rev. Lett. **59** (1987), 627 doi:10.1103/PhysRevLett.59.627
[3] N. Konno, H. Nakamura and H. Noya, Phys. Rev. D **37**, 154-158 (1988) doi:10.1103/PhysRevD.37.154
[4] M. Oka, Phys. Rev. D **38**, 298 (1988) doi:10.1103/PhysRevD.38.298
[5] V. B. Kopeliovich, B. Schwesinger and B. E. Stern, Nucl. Phys. A **549**, 485-497 (1992) doi:10.1016/0375-9474(92)90661-3
[6] F. Wang, J. I. Ping, G. h. Wu, L. j. Teng and J. T. Goldman, Phys. Rev. C **51**, 3411 (1995) doi:10.1103/PhysRevC.51.3411

[arXiv:nucl-th/9512014 [nucl-th]].
[7] Z. Y. Zhang, Y. W. Yu, C. R. Ching, T. H. Ho and Z. D. Lu, Phys. Rev. C **61**, 065204 (2000) doi:10.1103/PhysRevC.61.065204
[8] G. H. Wu, L. J. Teng, J. L. Ping, F. Wang and J. T. Goldman, Phys. Rev. C **53**, 1161-1166 (1996) doi:10.1103/PhysRevC.53.1161
[9] F. Wang, G. h. Wu, L. j. Teng and J. T. Goldman, Phys. Rev. Lett. **69**, 2901-2904 (1992) doi:10.1103/PhysRevLett.69.2901 [arXiv:nucl-th/9210002 [nucl-th]].
[10] L. Chen, H. Pang, H. Huang, J. Ping and F. Wang, Phys. Rev. C **76**, 014001 (2007) doi:10.1103/PhysRevC.76.014001 [arXiv:nucl-th/0703103 [nucl-th]].

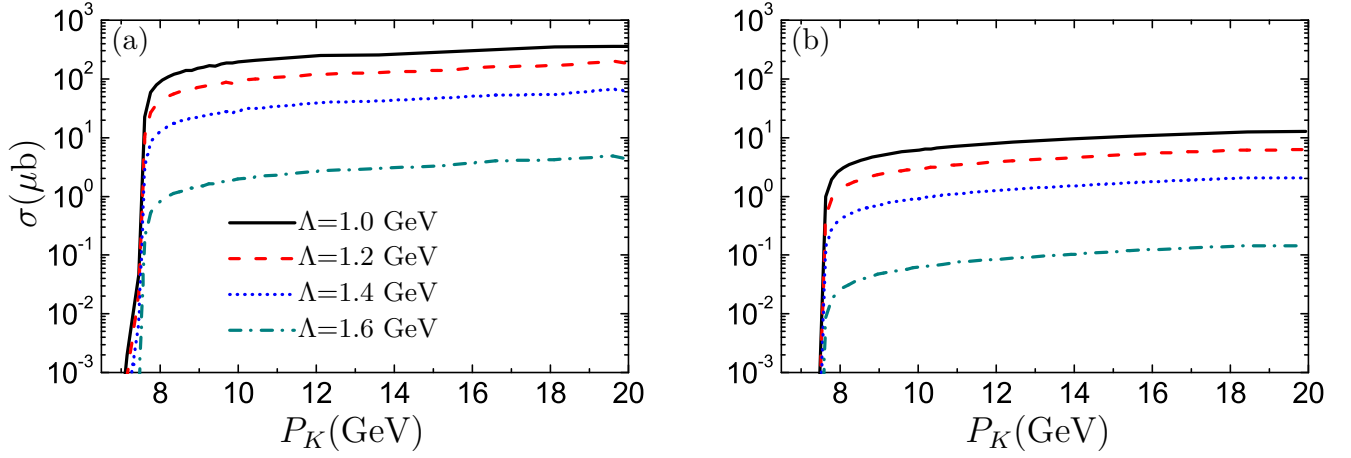


FIG. 7: The same as Fig. 6 but with the form factor in Mode II.

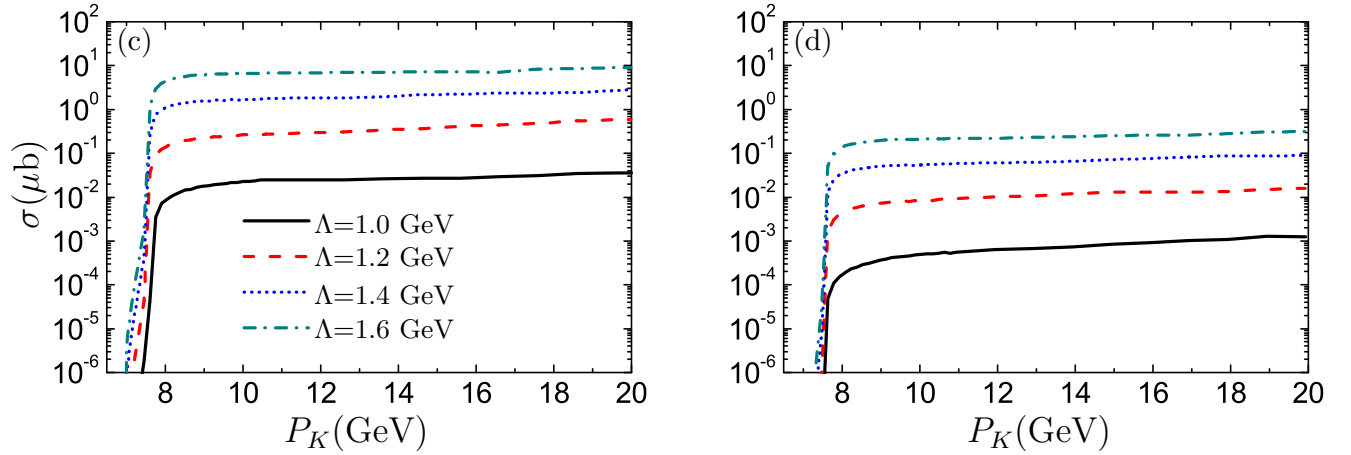


FIG. 8: The same as Fig. 6 but with the form factor in Mode III.

- [11] J. I. Ping, F. Wang and J. T. Goldman, Nucl. Phys. A **688**, 871-881 (2001) doi:10.1016/S0375-9474(00)00593-5 [arXiv:nucl-th/0007040 [nucl-th]].
- [12] H. r. Pang, J. I. Ping, F. Wang, J. T. Goldman and E. g. Zhao, Phys. Rev. C **69**, 065207 (2004) doi:10.1103/PhysRevC.69.065207 [arXiv:nucl-th/0306043 [nucl-th]].
- [13] F. Froemel, B. Julia-Diaz and D. O. Riska, Nucl. Phys. A **750**, 337-356 (2005) doi:10.1016/j.nuclphysa.2005.01.022 [arXiv:nucl-th/0410034 [nucl-th]].
- [14] B. Julia-Diaz and D. O. Riska, Nucl. Phys. A **755**, 431-434 (2005) doi:10.1016/j.nuclphysa.2005.03.050 [arXiv:nucl-th/0405061 [nucl-th]].
- [15] L. R. Dai, D. Zhang, C. R. Li and L. Tong, [arXiv:nucl-th/0606056 [nucl-th]].
- [16] M. Bashkanov, C. Bargholtz, M. Berlowski, D. Bogoslawsky, H. Calen, H. Clement, L. Demiroers, E. Doroshkevich, D. Duniec and C. Ekstrom, *et al.* Phys. Rev. Lett. **102**, 052301 (2009) doi:10.1103/PhysRevLett.102.052301 [arXiv:0806.4942 [nucl-ex]].
- [17] P. Adlarson *et al.* [WASA-at-COSY], Phys. Rev. Lett. **106**, 242302 (2011) doi:10.1103/PhysRevLett.106.242302 [arXiv:1104.0123 [nucl-ex]].
- [18] P. Adlarson *et al.* [WASA-at-COSY], Phys. Lett. B **721** (2013), 229-236 doi:10.1016/j.physletb.2013.03.019 [arXiv:1212.2881 [nucl-ex]].
- [19] P. Adlarson *et al.* [WASA-at-COSY], Phys. Rev. C **88**, no.5, 055208 (2013) doi:10.1103/PhysRevC.88.055208 [arXiv:1306.5130 [nucl-ex]].
- [20] P. Adlarson *et al.* [WASA-at-COSY], Phys. Lett. B **743**, 325-332 (2015) doi:10.1016/j.physletb.2015.02.067 [arXiv:1409.2659 [nucl-ex]].
- [21] P. Adlarson *et al.* [WASA-at-COSY], Phys. Rev. C **91**, no.1, 015201 (2015) doi:10.1103/PhysRevC.91.015201 [arXiv:1408.5744 [nucl-ex]].
- [22] P. Adlarson *et al.* [WASA-at-COSY], Phys. Rev. Lett. **112** (2014) no.20, 202301 doi:10.1103/PhysRevLett.112.202301 [arXiv:1402.6844 [nucl-ex]].
- [23] P. P. Shi, F. Huang and W. L. Wang, Eur. Phys. J. C **79** (2019) no.4, 314 doi:10.1140/epjc/s10052-019-6809-1 [arXiv:1904.06018 [nucl-th]].
- [24] F. Huang, Z. Y. Zhang, P. N. Shen and W. L. Wang, Chin. Phys. C **39** (2015) no.7, 071001 doi:10.1088/1674-1137/39/7/071001 [arXiv:1408.0458 [nucl-th]].
- [25] Y. Dong, P. Shen, F. Huang and Z. Zhang, Phys. Rev. C **91** (2015) no.6, 064002 doi:10.1103/PhysRevC.91.064002 [arXiv:1503.02456 [nucl-th]].
- [26] Y. Dong, F. Huang, P. Shen and Z. Zhang, Phys. Rev.

- C **94** (2016) no.1, 014003 doi:10.1103/PhysRevC.94.014003 [arXiv:1603.08748 [hep-ph]].
- [27] Y. Dong, F. Huang, P. Shen and Z. Zhang, Phys. Lett. B **769** (2017), 223-226 doi:10.1016/j.physletb.2017.03.058 [arXiv:1702.03658 [nucl-th]].
- [28] F. Huang, P. N. Shen, Y. B. Dong and Z. Y. Zhang, Sci. China Phys. Mech. Astron. **59**, no.2, 622002 (2016) doi:10.1007/s11433-015-5767-3 [arXiv:1505.05395 [nucl-th]].
- [29] S. Gongyo *et al.* [HAL QCD], Phys. Lett. B **811**, 135935 (2020) doi:10.1016/j.physletb.2020.135935 [arXiv:2006.00856 [hep-lat]].
- [30] F. Huang, Rev. Mex. Fis. Suppl. **3**, no.3, 0308031 (2022) doi:10.31349/SuplRevMexFis.3.0308031
- [31] N. Ikeno, R. Molina and E. Oset, Phys. Rev. C **104** (2021) no.1, 014614 doi:10.1103/PhysRevC.104.014614 [arXiv:2103.01712 [nucl-th]]. Copy to ClipboardDownload
- [32] R. Molina, N. Ikeno and E. Oset, [arXiv:2102.05575 [nucl-th]].
- [33] R. Molina, N. Ikeno and E. Oset, [arXiv:2209.10459 [nucl-th]].
- [34] A. Gal and H. Garcilazo, Nucl. Phys. A **928** (2014), 73-88 doi:10.1016/j.nuclphysa.2014.02.019 [arXiv:1402.3171 [nucl-th]].
- [35] W. Meguro, Y. R. Liu and M. Oka, Phys. Lett. B **704**, 547-550 (2011) doi:10.1016/j.physletb.2011.09.088 [arXiv:1105.3693 [hep-ph]].
- [36] Y. R. Liu and M. Oka, Phys. Rev. D **85**, 014015 (2012) doi:10.1103/PhysRevD.85.014015 [arXiv:1103.4624 [hep-ph]].
- [37] H. Huang, J. Ping and F. Wang, Phys. Rev. C **89**, no.3, 035201 (2014) doi:10.1103/PhysRevC.89.035201 [arXiv:1311.4732 [hep-ph]].
- [38] H. Huang, J. Ping and F. Wang, Phys. Rev. C **87**, no.3, 034002 (2013) doi:10.1103/PhysRevC.87.034002
- [39] Z. Liu, H. T. An, Z. W. Liu and X. Liu, Phys. Rev. D **105**, no.3, 034006 (2022) doi:10.1103/PhysRevD.105.034006 [arXiv:2112.02510 [hep-ph]].
- [40] Z. T. Lu, H. Y. Jiang and J. He, Phys. Rev. C **102**, no.4, 045202 (2020) doi:10.1103/PhysRevC.102.045202 [arXiv:2007.15878 [nucl-th]].
- [41] X. H. Chen, Q. N. Wang, W. Chen and H. X. Chen, Chin. Phys. C **45**, no.4, 041002 (2021) doi:10.1088/1674-1137/abdfbe [arXiv:1906.11089 [hep-ph]].
- [42] H. Mutuk and K. Azizi, Phys. Rev. D **105**, no.9, 094021 (2022) doi:10.1103/PhysRevD.105.094021 [arXiv:2204.03050 [hep-ph]].
- [43] N. Brambilla, H. X. Chen, A. Esposito, J. Ferretti, A. Francis, F. K. Guo, C. Hanhart, A. Hosaka, R. L. Jaffe and M. Karliner, *et al.* [arXiv:2203.16583 [hep-ph]].
- [44] Q. B. Li and P. N. Shen, Eur. Phys. J. A **8**, 417-421 (2000) doi:10.1007/s100530050052 [arXiv:nucl-th/9910060 [nucl-th]].
- [45] X. H. Chen, Q. N. Wang, W. Chen and H. X. Chen, Phys. Rev. D **103** (2021) no.9, 094011 doi:10.1103/PhysRevD.103.094011 [arXiv:2103.09739 [hep-ph]].
- [46] F. Etminan *et al.* [HAL QCD], Nucl. Phys. A **928** (2014), 89-98 doi:10.1016/j.nuclphysa.2014.05.014 [arXiv:1403.7284 [hep-lat]].
- [47] S. Zhang and Y. G. Ma, Phys. Lett. B **811** (2020), 135867 doi:10.1016/j.physletb.2020.135867 [arXiv:2007.11170 [hep-ph]].
- [48] C. J. Xiao, Y. B. Dong, T. Gutsche, V. E. Lyubovitskij and D. Y. Chen, Phys. Rev. D **101**, 114032 (2020) doi:10.1103/PhysRevD.101.114032 [arXiv:2004.12415 [hep-ph]].
- [49] J. Adam *et al.* [STAR], Phys. Lett. B **790**, 490-497 (2019) doi:10.1016/j.physletb.2019.01.055 [arXiv:1808.02511 [hep-ex]].
- [50] S. Acharya *et al.* [ALICE], Nature **588** (2020), 232-238 [erratum: Nature **590** (2021), E13] doi:10.1038/s41586-020-3001-6 [arXiv:2005.11495 [nucl-ex]].
- [51] K. Aoki, H. Fujioka, T. Gogami, Y. Hidaka, E. Hiya, R. Honda, A. Hosaka, Y. Ichikawa, M. Ieiri and M. Isaka, *et al.* [arXiv:2110.04462 [nucl-ex]].
- [52] T. Nagae, The J-PARC project, Nucl. Phys. A **805**, 486 (2008).
- [53] F. Nerling [COMPASS Collaboration], Hadron Spectroscopy with COMPASS: Newest Results, EPJ Web Conf. **37** (2012) 01016.
- [54] V. Obraztsov [OKA Collaboration], High statistics measurement of the $K^+ \rightarrow \pi^0 e^+ \nu(\text{Ke3})$ decay formfactors, Nucl. Part. Phys. Proc. **273-275**, 1330 (2016).
- [55] B. Velghe [NA62-RK and NA48/2 Collaborations], $K^\pm \rightarrow \pi^\pm \gamma \gamma$ Studies at NA48/2 and NA62-RK Experiments at CERN, Nucl. Part. Phys. Proc. **273-275**, 2720 (2016).
- [56] J. Liu, Q. Wu, J. He, D. Y. Chen and T. Matsuki, Phys. Rev. D **101** (2020) no.1, 014003 doi:10.1103/PhysRevD.101.014003 [arXiv:2001.00212 [hep-ph]].
- [57] J. Liu, D. Y. Chen and J. He, Eur. Phys. J. C **81** (2021) no.11, 965 doi:10.1140/epjc/s10052-021-09766-6 [arXiv:2108.00148 [hep-ph]].
- [58] X. H. Liu, Q. Zhao and F. E. Close, Phys. Rev. D **77** (2008), 094005 doi:10.1103/PhysRevD.77.094005 [arXiv:0802.2648 [hep-ph]].
- [59] Y. Huang, J. He, X. Liu, H. F. Zhang, J. J. Xie and X. R. Chen, Phys. Rev. D **93** (2016) no.3, 034022 doi:10.1103/PhysRevD.93.034022 [arXiv:1512.00981 [hep-ph]].
- [60] D. Ronchen, M. Doring, F. Huang, H. Haberzettl, J. Haidenbauer, C. Hanhart, S. Krewald, U. G. Meissner and K. Nakayama, Eur. Phys. J. A **49**, 44 (2013) doi:10.1140/epja/i2013-13044-5 [arXiv:1211.6998 [nucl-th]].
- [61] J. He, Phys. Rev. D **95**, no.7, 074031 (2017) doi:10.1103/PhysRevD.95.074031 [arXiv:1701.03738 [hep-ph]].
- [62] R. Machleidt, K. Holinde and C. Elster, Phys. Rept. **149**, 1-89 (1987) doi:10.1016/S0370-1573(87)80002-9
- [63] A. Matsuyama, T. Sato and T. S. H. Lee, Phys. Rept. **439**, 193-253 (2007) doi:10.1016/j.physrep.2006.12.003 [arXiv:nucl-th/0608051 [nucl-th]].
- [64] W. Liu, C. M. Ko and Z. W. Lin, Phys. Rev. C **65**, 015203 (2002) doi:10.1103/PhysRevC.65.015203
- [65] C. Schutz, J. W. Durso, K. Holinde and J. Speth, Phys. Rev. C **49** (1994), 2671-2687 doi:10.1103/PhysRevC.49.2671
- [66] B. Renner, Phys. Lett. B **33** (1970), 599-600 doi:10.1016/0370-2693(70)90359-X Copy to ClipboardDownload
- [67] J. He and D. Y. Chen, Eur. Phys. J. C **79** (2019) no.11, 887 doi:10.1140/epjc/s10052-019-7419-7 [arXiv:1909.05681 [hep-ph]].
- [68] D. Y. Chen, X. Liu and T. Matsuki, Phys. Rev. D **87** (2013) no.9, 094010 doi:10.1103/PhysRevD.87.094010 [arXiv:1304.0372 [hep-ph]].
- [69] D. Y. Chen, X. Liu and T. Matsuki, Phys. Rev. D **90** (2014) no.3, 034019 doi:10.1103/PhysRevD.90.034019 [arXiv:1406.6763 [hep-ph]].
- [70] N. A. Tornqvist, Nuovo Cim. A **107**, 2471-2476 (1994) doi:10.1007/BF02734018 [arXiv:hep-ph/9310225 [hep-ph]].
- [71] N. A. Tornqvist, Z. Phys. C **61**, 525-537 (1994) doi:10.1007/BF01413192 [arXiv:hep-ph/9310247 [hep-ph]].
- [72] M. P. Locher, Y. Lu and B. S. Zou, Z. Phys. A **347**, 281-284 (1994) doi:10.1007/BF01289796 [arXiv:nucl-th/9311021

[nucl-th]].

[73] X. Q. Li, D. V. Bugg and B. S. Zou, Phys. Rev. D **55**, 1421-1424

(1997) doi:10.1103/PhysRevD.55.1421